


 Cite this: *RSC Adv.*, 2018, **8**, 17847

 Received 31st March 2018  
 Accepted 4th May 2018

 DOI: 10.1039/c8ra02789g  
[rsc.li/rsc-advances](http://rsc.li/rsc-advances)

## Preparation and photo-induced activities of water-soluble amyloid $\beta$ -C<sub>60</sub> complexes†

 Naoki Hasunuma,<sup>a</sup> Masahiro Kawakami,<sup>a</sup> Hirotsugu Hiramatsu<sup>IP b</sup>  
 and Takakazu Nakabayashi<sup>ID, \*a</sup>

We have shown that fullerene (C<sub>60</sub>) becomes soluble in water by mixing fullerene and amyloid  $\beta$  peptide (A $\beta$ 40) whose fibril structures are considered to be associated with Alzheimer's disease. The water-solubility of fullerene arises from the generation of a nanosized complex between fullerene and the monomer species of A $\beta$ 40 (A $\beta$ 40-C<sub>60</sub>). The prepared A $\beta$ 40-C<sub>60</sub> exhibits photo-induced activity with visible light to induce the inhibition of A $\beta$ 40 fibrillation and the cytotoxicity for cultured HeLa cells. The observed photo-induced phenomena result from the generation of singlet oxygen *via* photoexcitation, inducing oxidative damage to A $\beta$ 40 and HeLa cells. The oxidized A $\beta$ 40 following photoexcitation of A $\beta$ 40-C<sub>60</sub> was confirmed by mass spectrometry.

### Introduction

Fullerene (C<sub>60</sub>) and its derivatives have received considerable attention over the last two decades due to their wide range of applications such as in photovoltaic and artificial photosynthetic devices.<sup>1–3</sup> In the field of medicine and biochemistry, much effort has been devoted to the application of fullerenes to photodynamic therapy (PDT) since fullerenes have the ability to efficiently generate singlet oxygen, which is one of the reactive oxygen species (ROS), upon photoexcitation.<sup>4–7</sup> Singlet oxygen is generated from energy transfer from the triplet excited state of C<sub>60</sub> to O<sub>2</sub> in the ground triplet state, and C<sub>60</sub> exhibits a very high quantum yield of the formation of the triplet state from the singlet excited state (~0.96 for C<sub>60</sub> in benzene<sup>8</sup>), resulting in the efficient generation of singlet oxygen. However, fullerenes are completely insoluble in water, which precludes their application to most biological systems. Chemical modifications such as the addition of hydroxyl groups have been performed to solubilize fullerenes in water.<sup>9–13</sup> Other methods such as the inclusion of organic macromolecules,<sup>14–16</sup> laser ablation,<sup>7,17</sup> and solvent substitution methods<sup>18</sup> have also been proposed. A variety of water-soluble fullerene derivatives have now been chemically synthesized; however, a sufficient amount of fullerene derivative seems not to be readily prepared in many cases. Simple methods for preparing sufficient amounts of water-soluble fullerenes are necessary for the purpose applying fullerenes to a variety of biochemical methodologies.

<sup>a</sup>Graduate School of Pharmaceutical Sciences, Tohoku University, Sendai 980-8578, Japan. E-mail: [takan@m.tohoku.ac.jp](mailto:takan@m.tohoku.ac.jp)

<sup>b</sup>Department of Applied Chemistry and Institute of Molecular Science, National Chiao Tung University, 1001, Ta-Hsueh Road, Hsinchu 30010, Taiwan

† Electronic supplementary information (ESI) available. See DOI: [10.1039/c8ra02789g](https://doi.org/10.1039/c8ra02789g)

In the present study, we have shown that C<sub>60</sub> becomes soluble in water simply by mixing C<sub>60</sub> and amyloid  $\beta$  1–40 (A $\beta$ 40) peptide in distilled water. A pale yellow aqueous solution was obtained just after stirring the mixture. The solubility of C<sub>60</sub> in water results from the generation of a complex between C<sub>60</sub> and A $\beta$  (A $\beta$ 40-C<sub>60</sub>). Herein, we have investigated (i) the generation, fundamental properties, and stability of A $\beta$ 40-C<sub>60</sub>, (ii) the inhibition of fibrillation of A $\beta$ 40 using A $\beta$ 40-C<sub>60</sub> and light, and (iii) the application of A $\beta$ 40-C<sub>60</sub> in PDT.

A $\beta$  peptides have extensively been studied due to their role in the development of Alzheimer's disease.<sup>19,20</sup> A $\beta$  peptides are generated from  $\beta$ -amyloid precursor protein, and the oligomeric and fibril forms of A $\beta$  have been reported to be toxic and causative agents in the pathogenesis of Alzheimer's disease. Therefore, investigations into the inhibition of A $\beta$  fibrillation from monomer peptides are important to suppress the progression of Alzheimer's disease.<sup>21–27</sup> If ROS generated by photoexcitation of fullerenes can be applied to A $\beta$ , there is a possibility that A $\beta$  fibrillation can be inhibited by fullerenes and light. Actually, the inhibition of A $\beta$  fibrillation by photo-irradiation of water-soluble fullerene derivatives was reported<sup>28,29</sup> and these fullerenes are expected to be fibril inhibitors like the photoactive compounds recently reported.<sup>30–33</sup> The present A $\beta$ 40-C<sub>60</sub> also exhibits the photo-induced activity to inhibit the fibrillation of A $\beta$ 40.

### Experimental

#### Preparation of A $\beta$ 40

A $\beta$ 40 was synthesized using a peptide synthesizer (431A, Applied Biosystems) and the crude product was purified with HPLC systems (JASCO) equipped with an ODP-50 column (Shodex). 5 mM ammonium acetate (pH 10.5) and acetonitrile



were used as hydrophilic and hydrophobic mobile phases, respectively. Molecular weight of the purified peptide determined by ESI mass spectrometry (solariX, Bruker) agreed with the monoisotopic mass of the A $\beta$ 40 peptide.<sup>34</sup>

The A $\beta$ 40 peptide was dissolved into doubly-distilled water (0.35 mg mL<sup>-1</sup>), and the solution was adjusted to pH 10.5 using an aqueous solution of NaOH. The solution was left at room temperature for 1 h to dissolve irregular and unexpected aggregates, and was then centrifuged (16 100 rcf, 10 min). The supernatant containing only the monomeric species of A $\beta$ 40 was diluted with an aqueous solution of NaOH (pH 10.5) and the concentration of A $\beta$ 40 was adjusted to 80  $\mu$ M using the molar absorption coefficient of a tyrosine residue of A $\beta$ 40 at 275 nm (1410 M<sup>-1</sup> cm<sup>-1</sup>).<sup>35</sup>

### Preparation of A $\beta$ 40-C<sub>60</sub> complex

2 mg of fullerene (C<sub>60</sub>) powder (Kanto Kagaku) was added to 1 mL of the aqueous solution of A $\beta$ 40 (80  $\mu$ M) at pH 10.5. The solution was stirred (*ca.* 800 rpm) at 4 °C for 120 h in a glass vial, followed by centrifugation (16 100 rcf, 10 min). The supernatant was collected and used as the solution of the A $\beta$ 40-C<sub>60</sub> complex. The concentration of C<sub>60</sub> in aqueous solution was in the range of 20–60  $\mu$ M. For the evaluation of the concentration, we used the peak of the absorption of A $\beta$ 40-C<sub>60</sub> at 342 nm with the assumption that its molar absorption coefficient is the same as that of the peak of the absorption of C<sub>60</sub> at 334 nm in *o*-dichlorobenzene ( $5.2 \times 10^4$  M<sup>-1</sup> cm<sup>-1</sup>).<sup>36</sup>

### Inhibitory effect on fibrillation of A $\beta$ 40

Sample solution was prepared by mixing 300  $\mu$ L of A $\beta$ 40-C<sub>60</sub> and/or A $\beta$ 40 aqueous solution and 300  $\mu$ L of buffer solution containing 40 mM Tris and 300 mM NaCl. The final concentration was  $\sim$ 40  $\mu$ M A $\beta$ 40 and 10–30  $\mu$ M C<sub>60</sub> with 20 mM Tris, 150 mM NaCl. To examine the effect of photoirradiation on the fibrillation of A $\beta$ 40, two sample tubes were separately prepared and incubated at 37 °C for 5 days. One was incubated without any pre-treatment, while the other was placed into a 1 cm quartz black cuvette and was irradiated with 488 nm cw laser light (Spectra-Physics) at 140 mW for 1 h in prior to the incubation. Fibrillation was monitored with measurements of circular dichroism (CD) and thioflavin T (ThT) fluorescence assay.

### Preparation of cells

HeLa cells were cultured in a 10 cm dish (Corning) filled with Dulbecco's Modified Eagle's Medium (DMEM) at 37 °C in the presence of 5% CO<sub>2</sub>. The cells were cultured until 80% confluent, and the cells were washed with phosphate buffered saline without Ca<sup>2+</sup> and Mg<sup>2+</sup> (PBS(–)) after removing DMEM. Then the HeLa cells were prepared with trypsin-EDTA treatment. After trypsin-EDTA was removed, DMEM was added to the dish, and the cell suspension was transferred to a centrifuge tube. DMEM was prepared as follows: Dulbecco's modified Eagle's medium (D5796, Sigma) was mixed with Fetal bovine serum (10 vol%) (10437-028, Gibco) and Penicillin G-Streptomycin sulfate (5 vol%) (15070-063, Gibco). PBS(–) containing NaCl (8.00 g L<sup>-1</sup>), KCl (0.20 g L<sup>-1</sup>), Na<sub>2</sub>HPO<sub>4</sub> (1.15 g L<sup>-1</sup>), and

KH<sub>2</sub>PO<sub>4</sub> (0.20 g L<sup>-1</sup>) was used for the experiments after autoclaving at 120 °C for 20 min.

### Thioflavin T fluorescence assay

30  $\mu$ L of aqueous solution including A $\beta$ 40-C<sub>60</sub> and/or A $\beta$ 40 was mixed with 1.3 mL of thioflavin T (ThT) solution containing 5  $\mu$ M ThT and 50 mM Gly-NaOH (pH 8.5), and left for 10 min at room temperature in dark to ensure the staining of A $\beta$ 40 fibrils. Then, the sample solution was placed in a 1 cm quartz cuvette and the fluorescence intensity at 485 nm was recorded for 3 min using a FP-6500 spectrofluorometer (JASCO). The excitation wavelength was 455 nm and the spectral slit width was set at 5 nm for both excitation and emission measurements. The average intensity for 3 min was plotted against the fibrillation reaction. To avoid sedimentation of insoluble aggregates, the sample solution was gently stirred with a stirrer in the cuvette during the measurement.

### ADPA absorption assay

Anthracene-9,10-dipropionic acid (ADPA) was commercially obtained from Chemodex Ltd. and was dissolved in aqueous solution whose pH was adjusted to pH 10.5 using an aqueous solution of NaOH. Then, 300  $\mu$ L of the prepared ADPA solution was mixed with the same amount (300  $\mu$ L) of A $\beta$ 40-C<sub>60</sub> aqueous solution and the final concentrations of ADPA and C<sub>60</sub> in the mixture were  $\sim$ 80  $\mu$ M and  $\sim$ 20  $\mu$ M, respectively. Then the mixed solution was placed into a 1 cm quartz black cuvette and was irradiated with 488 nm cw laser light (140 mW). The absorption spectrum of the solution was measured at each photo-irradiation time.

The yield of the generation of singlet oxygen ( $\Phi_{ROS}$ ) was estimated from the magnitude of the decrease in the absorption of ADPA at 399 nm (8300 M<sup>-1</sup> cm<sup>-1</sup>). The  $\Phi_{ROS}$  value of A $\beta$ 40-C<sub>60</sub> was estimated from that of rose bengal ( $\Phi_{ROS} = 0.76$  (ref. 37)) as a reference.

### Spectroscopic analyses

UV-vis absorption spectra were recorded using a U-3300 spectrophotometer (HITACHI) with a 1 cm quartz cuvette with black wall. Dynamic light scattering was measured using DynaPro-99 (Wyatt/ProteinSolutions) with a quartz cuvette of 3 mm optical path. CD spectra were recorded by a J-820 spectropolarimeter (JASCO, Japan) with a 0.5 mm quartz cell.

Electrospray ionization (ESI) mass spectra were measured using a solariX mass spectrometer (Bruker Daltonics). The lyophilized powder formed by the aqueous solution of A $\beta$ 40-C<sub>60</sub> with or without photoirradiation was dissolved in CH<sub>3</sub>CN-H<sub>2</sub>O (1 : 1, v/v) and their mass spectra were measured with the ESI method. The photoirradiation of the aqueous A $\beta$ 40-C<sub>60</sub> solution was performed in a 1 cm quartz cuvette with black wall with 488 nm cw laser light at 140 mW for 1 h as mentioned above.

The images of transmission electron microscope (TEM) were measured using a HF-2000 field-emission TEM (FE-TEM) (Hitachi) operating at 200 kV. The measurement sample was prepared by placing droplets of the sample aqueous solution on a copper grid and drying it in air.



## Viability of cells

100  $\mu$ L aliquots of the cell suspension ( $5 \times 10^3$  cells/100  $\mu$ L) were dispensed into the wells of two 96 well plates (thermo scientific). After incubation of the two plates at 37 °C for 24 h in 5% CO<sub>2</sub>, DMEM was replaced with 100  $\mu$ L Hanks' balanced salt solution (HBSS; H8264, Sigma) containing A $\beta$ 40-C<sub>60</sub> and/or A $\beta$ 40, whose pH was adjusted to 8.1. The final concentration of A $\beta$ 40 in each well for the test of A $\beta$ 40 only was  $\sim$ 16  $\mu$ M. For the test of A $\beta$ 40-C<sub>60</sub>, the final concentration of C<sub>60</sub> was 20  $\mu$ M in each well. The molar absorption coefficient of C<sub>60</sub> in *o*-dichlorobenzene was used for evaluating the concentration of C<sub>60</sub>, as mentioned above. One plate was irradiated with 30 W LED light for 2 h at 30 °C in the incubator (*i.e.*, the photoirradiated condition), while the other plate was shaded in a box and left at 30 °C for 2 h (*i.e.*, the dark condition). After the 2 h treatment, HBSS in each well was replaced with DMEM and the two plates were incubated for additional 18 h at 37 °C in 5% CO<sub>2</sub>. Then, 10  $\mu$ L of the solution of WST-8 dye (Cell count reagent SF, Nacalai Tesque) was added to each well and the cell viability was examined according to the protocol of the manufacturer. Absorbance at 450 nm was recorded using a plate reader (SpectraMax Paradigm, Molecular devices).

## Results

We have used A $\beta$ 40 (<sup>1</sup>DAEFRHDSGYEVHQKLVFFAEDVGSNK-GAIIGLMVGGVV<sup>40</sup>) as the amyloid peptide in the present study. This peptide constitutes  $\sim$ 90% of the secreted A $\beta$  peptides and is abundant in the brain.<sup>38,39</sup> Fig. S1 in ESI† shows the photograph of the aqueous solution of C<sub>60</sub> solubilized with A $\beta$ 40. Water-soluble C<sub>60</sub> was prepared only by adding C<sub>60</sub> into aqueous solution of purified A $\beta$ 40 at pH 10.5 and stirring the mixture for 5 days at 4 °C. Then the mixture was centrifuged and the supernatant solution with pale-yellow color (Fig. S1†) was obtained. Since C<sub>60</sub> is not dispersed in water without A $\beta$ 40, C<sub>60</sub> is solubilized in water with the interaction with A $\beta$ 40.

Fig. 1 shows the absorption spectra of prepared A $\beta$ 40-C<sub>60</sub> in water. All the observed bands arise from C<sub>60</sub> and the two bands at around 260 and 340 nm are the symmetry-allowed transitions to 6<sup>1</sup>T<sub>1u</sub> and 3<sup>1</sup>T<sub>1u</sub> from the ground state (1<sup>1</sup>A<sub>g</sub>), respectively.<sup>40,41</sup> The shape of the absorption spectrum is similar to that of C<sub>60</sub>;

however, the band shape becomes broader compared with that of the monomer species in heptane (Fig. S2†). The broadening of the absorption bands is generally observed with the formation of C<sub>60</sub> clusters in water prepared by the laser-ablation method,<sup>7,17</sup> encapsulation with natural protein surfactants,<sup>16</sup> and extended mixing.<sup>41</sup> The present result therefore indicates that A $\beta$ 40-C<sub>60</sub> molecules also exist as clusters encapsulated with A $\beta$ . The broadness of the cluster may come from the increase in electronic transition densities due to C<sub>60</sub>-C<sub>60</sub> and C<sub>60</sub>-water interactions and heterogeneity of the size and the shape of the cluster.<sup>41</sup> The visible absorption band that is assignable to intermolecular interactions between neighboring molecules in C<sub>60</sub> clusters<sup>17</sup> is also observed around 450 nm. It has been reported that the intensity of the visible band around 500 nm relative to that of the transition to 3<sup>1</sup>T<sub>1u</sub> ( $\sim$ 340 nm) increases with particle size.<sup>41</sup> The size of A $\beta$ 40-C<sub>60</sub> was estimated by dynamic light scattering to be 50–60 nm. The presence of A $\beta$ 40-C<sub>60</sub> clusters was also confirmed by TEM (Fig. S3†). The particles with a diameter of  $\sim$ 50 nm were observed in the TEM image. The number of C<sub>60</sub> constituting the cluster is  $\sim$ 3.5  $\times$  10<sup>5</sup> when the cluster has a diameter of 50 nm and a sphere.

The prepared A $\beta$ 40-C<sub>60</sub> was stable and even found to remain unchanged after one month at 4 °C, as shown by the constant shape and the intensity of the absorption spectrum after one month (Fig. 1). A $\beta$ 40-C<sub>60</sub> can also be used as a pale-yellow powder by lyophilization, and the powder can be re-dissolved in water (Fig. S1†).

A $\beta$ 40 has both hydrophobic and hydrophilic parts in a single chain and, therefore, it is conceivable that the hydrophobic part of A $\beta$ 40 interacts with C<sub>60</sub> and the hydrophilic part surrounds C<sub>60</sub>, resulting in solubilization and stabilization of C<sub>60</sub> in distilled water (Fig. S4†). The interactions between A $\beta$  peptides and fullerene were theoretically analyzed and it was proposed from molecular dynamics (MD) simulation that C<sub>60</sub> preferentially binds to a sequence of hydrophobic residues 16–20 KLVFF from the N terminus of A $\beta$ 40 or A $\beta$ 42.<sup>42,43</sup> A $\beta$ 40 in the prepared A $\beta$ 40-C<sub>60</sub> exists as monomer species having random structure, which was clarified by CD spectroscopy, as shown below.

We then investigated the application of A $\beta$ 40-C<sub>60</sub> to the phototherapy of disease. It should be noted that visible light at around 400–550 nm can be used as a photoirradiation source since C<sub>60</sub> clusters exhibit absorption in this region (Fig. 1). The photo-induced effects on the fibrillization of A $\beta$ 40 were investigated by the measurements of the CD spectra. A $\beta$ 40 forms the random structure in monomer species and the  $\beta$ -sheet structure in fibril, which can be distinguished by the shape of the CD spectrum. A $\beta$ 40 monomers turn into their fibril form when pH of the aqueous solution is set from basic (pH 10.5) to neutral (pH 7). Therefore, the effect of photoirradiation was examined by irradiation of 488 nm laser light to aqueous solution of A $\beta$ 40 just after changing pH to neutral. The irradiation time was 1 h.

The results of CD spectra of A $\beta$ 40 only are shown in panels A and B of Fig. 2. The secondary structure of a peptide can be determined by the shape of the CD spectrum: the CD spectrum exhibits a negative band at 195–200 nm in the random, a negative band around 215 nm and a positive band at 195–200 nm in the  $\beta$ -sheet, and a positive band at 195–200 nm and two negative

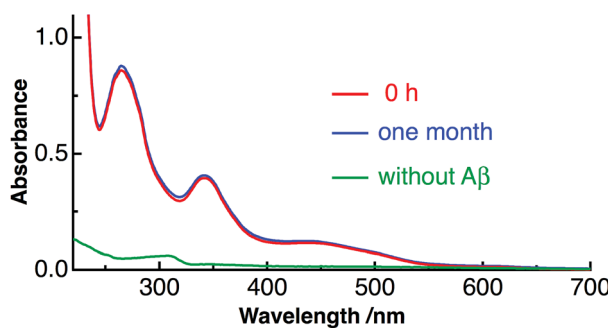


Fig. 1 Absorption spectra of A $\beta$ 40-C<sub>60</sub> in water just after preparation (red) and after one month at 4 °C (blue), together with the absorption spectrum of C<sub>60</sub> only in water (green).



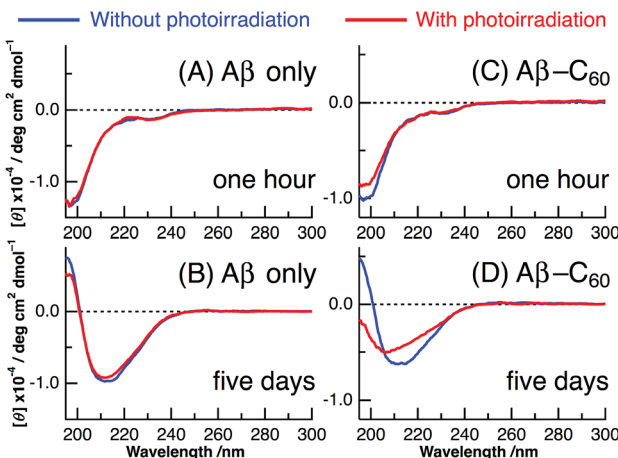


Fig. 2 CD spectra of A $\beta$ 40 only (A and B) and A $\beta$ 40-C<sub>60</sub> (C and D) after  $\sim$ 1 hour from the preparation (A and C) and after the incubation of 5 days (B and D) at 37 °C without photoirradiation (blue) and with photoirradiation at 488 nm (red).

peaks at 208 and 222 nm in the  $\alpha$ -helix. After  $\sim$ 1 h from the change to neutral condition, the CD spectrum of A $\beta$ 40 only exhibited the negative peak at  $\sim$ 198 nm irrespective of photoirradiation, which arises from the random structure of A $\beta$  monomer (Fig. 2A). On the other hand, after incubation at 37 °C for 5 days, the shape of the CD spectrum resembled that of the  $\beta$ -sheet structure with positive values at less than 200 nm and a negative peak at  $\sim$ 210 nm (Fig. 2B). This result indicates that the fibril structure completely occurred after the incubation of 5 days. The fibril formation of A $\beta$ 40 only was not affected by photoirradiation at 488 nm after the 5 days incubation.

Panels C and D of Fig. 2 show the CD spectra of A $\beta$ 40-C<sub>60</sub> with and without photoirradiation. The CD spectrum of aqueous solution containing A $\beta$ 40-C<sub>60</sub> also exhibited the negative peak at  $\sim$ 198 nm after 1 h from the change to neutral condition (Fig. 2C), indicating the dominance of random structure in A $\beta$ 40. After incubation for 5 days at 37 °C (Fig. 2D), the CD spectrum of A $\beta$ 40-C<sub>60</sub> without photoirradiation was changed to that of  $\beta$ -sheet structure, which is the same as that of A $\beta$ 40 only. However, upon photoirradiation, A $\beta$ 40-C<sub>60</sub> exhibited a different CD spectrum having negative values shorter than 200 nm and a negative peak at  $\sim$ 205 nm (Fig. 2D). This result indicates that the A $\beta$  fibril was not efficiently generated in the aqueous solution including A $\beta$ 40-C<sub>60</sub> upon photoirradiation at 488 nm. It can be considered that the random structure of A $\beta$ 40 still exists in the photoirradiated A $\beta$ 40-C<sub>60</sub> solution. Fig. 3 shows the decomposition analysis of the CD spectrum of A $\beta$ 40-C<sub>60</sub> after photoirradiation. The CD spectrum after photoirradiation was well fitted with the linear combination of those of the random and the  $\beta$ -sheet structure (Fig. 3). These results lead us to a conclusion that the fibril formation of A $\beta$ 40 is inhibited by A $\beta$ 40-C<sub>60</sub> upon photoirradiation. Since the A $\beta$  fibril was smoothly generated in the A $\beta$ 40-C<sub>60</sub> solution without photoirradiation (Fig. 2D), A $\beta$ 40-C<sub>60</sub> alone has no ability to inhibit the fibril formation with the present C<sub>60</sub> concentration, and photoirradiation is necessary to block the fibril formation using A $\beta$ 40-C<sub>60</sub>.

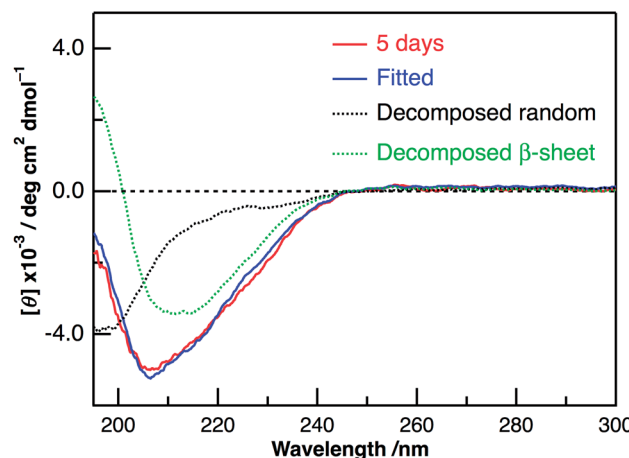


Fig. 3 The observed (red) and fitted (blue) CD spectra of A $\beta$ 40-C<sub>60</sub> after the incubation for 5 days at 37 °C with photoirradiation at 488 nm, together with the deconvoluted CD spectra of the random (black) and  $\beta$ -sheet (green) structures obtained by the fitting procedure. The CD spectrum of A $\beta$ 40-C<sub>60</sub> just after the preparation with photoirradiation and that of A $\beta$ 40-C<sub>60</sub> after the incubation of 5 days at 37 °C without photoirradiation were used as those of the random and  $\beta$ -sheet structures, respectively.

The inhibition on the fibril formation by photoirradiated A $\beta$ 40-C<sub>60</sub> is also confirmed by ThT fluorescence that exhibits strong fluorescence when A $\beta$  peptides form fibril structures. We have measured the intensity of ThT fluorescence of the solutions of A $\beta$ 40 only and A $\beta$ 40-C<sub>60</sub>, respectively, after incubation for 5 days at 37 °C (Fig. 4). The ThT fluorescence of the solution of A $\beta$ 40 only remained unchanged upon photoirradiation, confirming the negligible effect of the photoirradiation in absence of C<sub>60</sub>. The ThT fluorescence of the solution of A $\beta$ 40-C<sub>60</sub> without photoirradiation exhibited the similar intensity to those of A $\beta$ 40 only. This result indicates that the fibril formation was not affected solely by the addition of A $\beta$ 40-C<sub>60</sub> in the present concentration. On the other hand, the intensity of A $\beta$ 40-C<sub>60</sub> upon photoirradiation was markedly weaker than those of the other solutions, confirming the suppression of the fibril formation by photoirradiated A $\beta$ 40-C<sub>60</sub>. In conclusion, all the

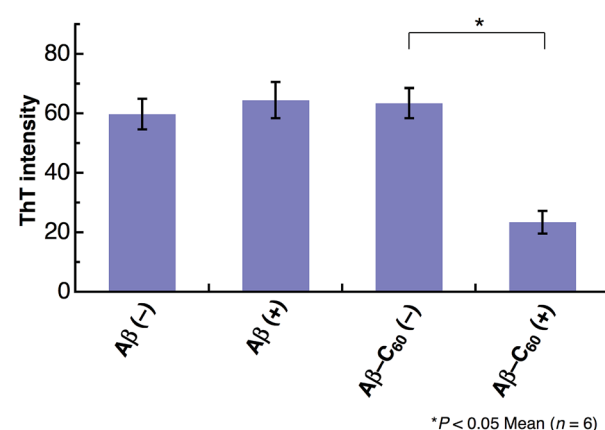


Fig. 4 ThT fluorescence after 5 days incubation of A $\beta$ 40 or A $\beta$ 40-C<sub>60</sub>. The experiments without photoirradiation are shown as (–). The wavelength of photoirradiation was 488 nm.

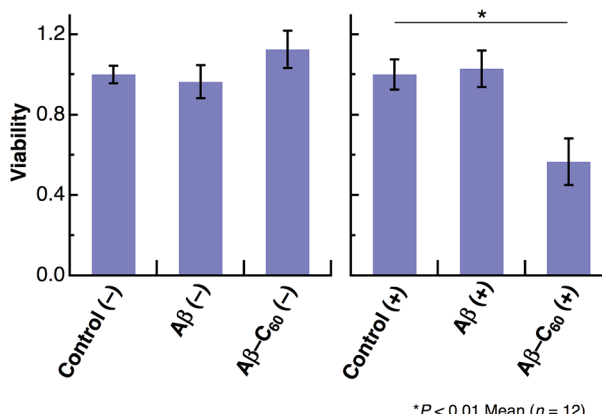


Fig. 5 Viability of HeLa cells treated with A $\beta$ 40 or A $\beta$ 40-C<sub>60</sub> relative to untreated control with or without photoirradiation. The experiments without photoirradiation are shown as (-). The wavelength range of photoirradiation was 400–700 nm.

obtained results indicate that A $\beta$ 40-C<sub>60</sub> inhibits the formation of the amyloid fibril with photoirradiation.

We further studied the induction of cell death using A $\beta$ 40-C<sub>60</sub>. HeLa cells were incubated in a 96-well plate with A $\beta$ 40 or A $\beta$ 40-C<sub>60</sub> and the extent of cell death was evaluated by the WST-8 assay. A visible diode lamp was used as a photoirradiation source. Fig. 5 shows the cytotoxicity results for A $\beta$ 40 and A $\beta$ 40-C<sub>60</sub>, which were evaluated by estimating the number of living cells relative to the untreated control with or without photoirradiation. The viability of HeLa cells remained almost unchanged upon introducing A $\beta$ 40 or A $\beta$ 40-C<sub>60</sub>, indicating that the toxicity of A $\beta$ 40-C<sub>60</sub> itself was similar to that of A $\beta$ 40 only. The effect of photoirradiation was only observed in A $\beta$ 40-C<sub>60</sub>; the viability decreased to *ca.* 60% upon application of A $\beta$ 40-C<sub>60</sub> with photoirradiation. This result indicates that A $\beta$ 40-C<sub>60</sub> induces cell death only with the photoirradiation. The photo-induced reduction of the viability of cells demonstrates the applicability of A $\beta$ 40-C<sub>60</sub> to PDT.

## Discussion

In the present study, we have shown that C<sub>60</sub> is solubilized in water only by mixing with A $\beta$ 40 and that the prepared water-soluble A $\beta$ 40-C<sub>60</sub> exhibits the efficient inhibition of the fibril formation and the cytotoxicity inducing cell death upon photoirradiation with visible light. These phenomena are considered to arise from singlet oxygen generated *via* photoexcitation of A $\beta$ 40-C<sub>60</sub>, which comes from the fact that singlet oxygen is generated by photoexcitation of C<sub>60</sub>, as mentioned in Introduction. The existence of oxidized species after photoirradiation can be confirmed by mass spectrometry.

Fig. 6 shows the ESI mass spectra of A $\beta$ 40-C<sub>60</sub> before and after photoirradiation. In Fig. 6A, the peak at 866.44 both before and after photoirradiation is assigned to the pentavalent charged peptide (C<sub>194</sub>H<sub>295</sub>N<sub>53</sub>O<sub>58</sub>S + 5H<sup>+</sup>) and the other main peaks at 722.20 and 1082.79 are assigned to the different charge states, +6 and +4, respectively. In the spectrum after the photoirradiation (Fig. 6B), the monoisotopic mass of 4341.2 is

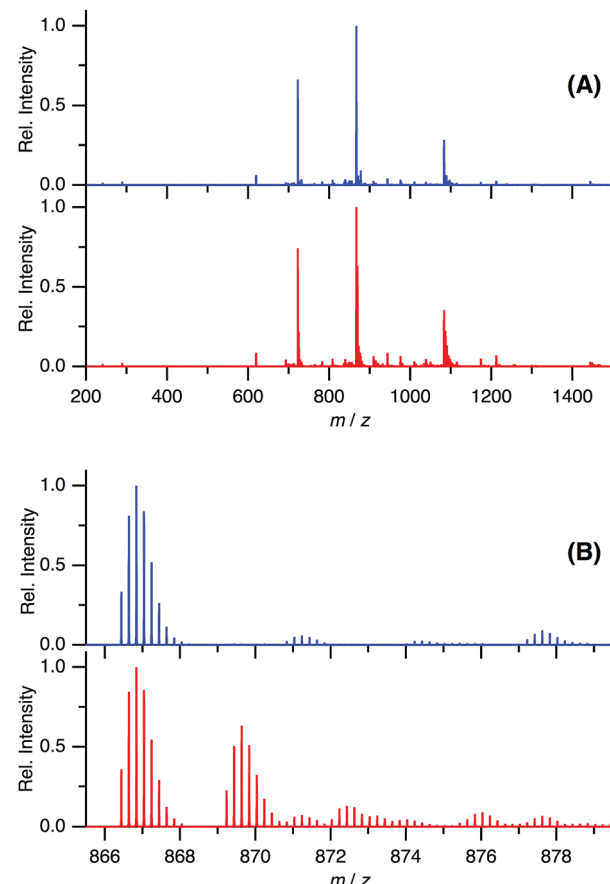


Fig. 6 ESI-mass spectra of A $\beta$ 40-C<sub>60</sub> without (blue) and with (red) photoirradiation at *m/z* 200–1500 (A) and 865.5–879.5 (B). The wavelength of photoirradiation was 488 nm.

ascribed to the oxidized peptide (C<sub>194</sub>H<sub>295</sub>N<sub>53</sub>O<sub>58</sub>S + O – 2H) and those of 4355.2 and 4373.2 are the peptides where two sites (C<sub>194</sub>H<sub>295</sub>N<sub>53</sub>O<sub>58</sub>S + 2O – 4H) and three sites (C<sub>194</sub>H<sub>295</sub>N<sub>53</sub>O<sub>58</sub>S + 3O – 2H) are oxidized, respectively. All these peaks were not observed in the spectrum without photoirradiation. The peaks assignable to oxidized species in Fig. 6B were not observed in the mass spectra of A $\beta$ 40 only after photoirradiation (Fig. S5†). These results lead us to a conclusion that the oxidized A $\beta$ 40 peptide exists only in A $\beta$ 40-C<sub>60</sub> solution with the photoirradiation. It is conceivable that the oxidized species with (–2H + O) and (–4H + 2O) come from the oxidation of the serine and histidine residues that are easily oxidized among amino acids; however, non-specific oxidation of other residues should also be considered because of the existence of the species with (–2H + 3O). These oxidation processes result in the suppression of the fibril formation.

Only one residue alternation in A $\beta$  has been shown to affect the ability of the fibrillation.<sup>34,44–46</sup> It has been systematically studied for the effect of one mutation of A $\beta$  on the fibril formation:<sup>44,45</sup> the magnitude of the fibrillation depends on the position and the amino acid of the mutation. The oxidation of methionine was also reported to inhibit A $\beta$  fibrillation.<sup>46</sup> The fibrillation is proceeded *via* hydrophobic and electrostatic interactions among peptides, and the fibrillation rate depends



on the absolute value of the charges.<sup>45</sup> Therefore, it is conceivable that the change in the interaction among peptides due to oxygen addition results in the change in the rate or the magnitude of the A $\beta$  fibrillation.

We also performed the ROS assay of A $\beta$ 40-C<sub>60</sub> using the absorption of anthracene-dipropionic acid (ADPA). The absorption of anthracene moiety of ADPA is reduced by the oxidation of ADPA with ROS species, and can be used to quantify ROS.<sup>15</sup> The  $\Phi_{ROS}$  value of A $\beta$ 40-C<sub>60</sub> was estimated from the magnitude of the decrease in the absorption of ADPA with photoexcitation of A $\beta$ 40-C<sub>60</sub> (Fig. 7). The same experiment was also performed for rose bengal with the same excitation wavelength as a reference ( $\Phi_{ROS} = 0.76$  (ref. 37)), and  $\Phi_{ROS}$  of A $\beta$ 40-C<sub>60</sub> was calculated from the number of absorbed photon and the magnitude of the photo-induced decrease for both the solutions. A decrease in the absorbance of ADPA was observed with the inclusion of A $\beta$ 40-C<sub>60</sub> and photoirradiation. Since the absorbance of ADPA without A $\beta$ 40-C<sub>60</sub> remained constant upon photoirradiation, the observed decrease in the ADPA absorption

can be ascribed to the generation of ROS *via* photoexcitation of A $\beta$ 40-C<sub>60</sub>. The yield of the ROS generation was qualitatively estimated to be  $\sim 0.05$  (Fig. 7), which is lower than that of C<sub>60</sub> monomer. The magnitude of photo-induced cell death of the present A $\beta$ 40-C<sub>60</sub> was lower than those of other water-soluble fullerenes,<sup>47,48</sup> which may also be due to the small value of  $\Phi_{ROS}$ . The low yield of the ROS generation is thought to arise from the cluster structure; the yield of intersystem crossing of C<sub>60</sub> remarkably decreases with cluster formation.<sup>7,17</sup> The yield of the triplet formation may depend on the cluster size<sup>7</sup> and the decrease in the lifetime of the singlet state with the cluster formation prevents the relaxation to the triplet state.<sup>17</sup> The consumption of ROS to the oxidation of the attached peptides should also be considered. We are in progress to prepare A $\beta$ 40-C<sub>60</sub> with smaller sizes by controlling the mixture time and the stirring speed to increase the efficiency of the ROS generation.

The present result for solubilizing C<sub>60</sub> in water provides a method of preparation of a sufficient amount of water-soluble A $\beta$ 40-C<sub>60</sub>. The water-soluble C<sub>60</sub> clusters are also prepared by the laser ablation<sup>7,17</sup> and the solvent substitution methods.<sup>18</sup> However, the C<sub>60</sub> clusters prepared by laser ablation are not generally protected by macromolecules such as the present A $\beta$ 40, and therefore the precipitation of C<sub>60</sub> inevitably occurs in buffer solutions (the solutions including large amounts of electrolytes). In the solvent substitution method, trace amounts of residual organic solvent may affect the condition of cultured cells. The present method is applicable to buffer solutions and no organic solvent is used during the preparation, which are the advantage of the present method. Furthermore, the most important point of the present method with regards to the fibril inhibition is that A $\beta$  peptide itself acts as a surfactant for the C<sub>60</sub> clusters. No other compound is necessary and A $\beta$  peptide smoothly interacts with other A $\beta$  peptides. The present A $\beta$ 40-C<sub>60</sub> can be considered to strongly interact with other A $\beta$  peptides, resulting in the photo-induced inhibition of the fibril formation.

## Conclusion

It has been shown that C<sub>60</sub> becomes soluble in water by forming the complex with A $\beta$  peptides. The prepared complex exhibits the photo-induced activity to induce the inhibition of the A $\beta$  fibrillation and cell death by the generation of singlet oxygen upon photoirradiation. It is also conceivable that other peptides with hydrophobic and hydrophilic parts in a chain can be used to solubilize C<sub>60</sub> in water. In future studies, the preparation of very small C<sub>60</sub> clusters using other peptides will be examined. Finally, we believe that the present water-solubilization method using peptides will expand the application potential of the photo-induced phenomena of fullerenes and other carbon materials to a variety of biological systems.

## Conflicts of interest

There are no conflicts to declare.

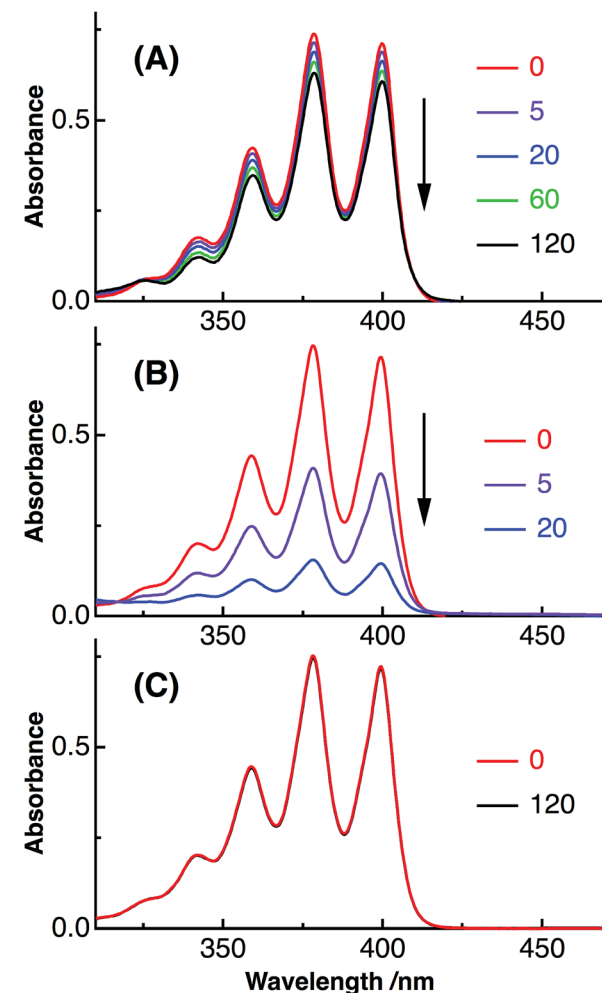


Fig. 7 Absorption spectra of ADPA with A $\beta$ 40-C<sub>60</sub> (A) and rose bengal (B) after the photoirradiation. The irradiation time was shown on the right of each figure. Absorption spectra of ADPA only are also shown in (C) as a control. The wavelength of photoirradiation was 488 nm for both (A) and (B).

## Acknowledgements

The authors thank Dr Yasuhiko Kasama (Idea International Co. Ltd) and Prof. Eunsang Kwon (Tohoku University) for their valuable comments.

## Notes and references

- 1 C. G. Shuttle, R. Hamilton, B. C. O'Regan, J. Nelson and J. R. Durrant, *Proc. Natl. Acad. Sci. U. S. A.*, 2010, **107**, 16448.
- 2 Y. Li, *Acc. Chem. Res.*, 2012, **45**, 723.
- 3 Y. Tachibana, L. Vayssieres and J. R. Durrant, *Nat. Photonics*, 2012, **6**, 511.
- 4 Y. Yamakoshi, N. Umezawa, A. Ryu, K. Arakane, N. Miyata, Y. Goda, T. Masumizu and T. Nagano, *J. Am. Chem. Soc.*, 2003, **125**, 12803.
- 5 P. Mroz, G. P. Tegos, H. Gali, T. Wharton, T. Sarna and M. R. Hamblin, *Photochem. Photobiol. Sci.*, 2007, **6**, 1139.
- 6 A. Ikeda, M. Akiyama, T. Ogawa and T. Takeya, *ACS Med. Chem. Lett.*, 2010, **1**, 115.
- 7 K. Ohkubo, N. Kohno, Y. Yamada and S. Fukuzumi, *Chem. Commun.*, 2015, **51**, 8082.
- 8 J. W. Arbogast, A. P. Darmany, C. S. Foote, Y. Rubin, F. N. Diederich, M. M. Alvarez, S. J. Anz and R. L. Whetten, *J. Phys. Chem.*, 1991, **95**, 11.
- 9 E. Nakamura and H. Isobe, *Acc. Chem. Res.*, 2003, **36**, 807.
- 10 S. Bosi, T. Da Ros, G. Spalluto and M. Prato, *Eur. J. Med. Chem.*, 2003, **38**, 913.
- 11 C. M. Sayes, J. D. Fortner, W. Guo, D. Lyon, A. M. Boyd, K. D. Ausman, Y. J. Tao, B. Sitharaman, L. J. Wilson, J. B. Hughes, J. L. West and V. L. Colvin, *Nano Lett.*, 2004, **4**, 1881.
- 12 K. Kokubo, K. Matsubayashi, H. Tategaki, H. Takada and T. Oshima, *ACS Nano*, 2008, **2**, 327.
- 13 F. Giacalone and N. Martín, *Adv. Mater.*, 2010, **22**, 4220.
- 14 A. McNally, R. J. Forster and T. E. Keyes, *Phys. Chem. Chem. Phys.*, 2009, **11**, 848.
- 15 T. Ohata, K. Ishihara, Y. Iwasaki, A. Sangsuwan, S. Fujii, K. Sakurai, Y. Ohara and S. Yusa, *Polym. J.*, 2016, **48**, 999.
- 16 S. J. Vance, V. Desai, B. O. Smith, M. W. Kennedy and A. Cooper, *Biophys. Chem.*, 2016, **214–215**, 27.
- 17 Y. Ishibashi, M. Arinishi, T. Katayama, H. Miyasaka and T. Asahi, *Chem. Lett.*, 2012, **41**, 1104.
- 18 S. Deguchi, R. G. Alargova and K. Tsujii, *Langmuir*, 2001, **17**, 6013.
- 19 M. P. Mattson, *Nature*, 2004, **430**, 631.
- 20 C. Iadecola, *Nat. Rev. Neurosci.*, 2004, **5**, 347.
- 21 M. Bartolini, C. Bertucci, V. Cavrini and V. Andrisano, *Biochem. Pharmacol.*, 2003, **65**, 407.
- 22 M. Citron, *Nat. Rev. Neurosci.*, 2004, **5**, 677.
- 23 C. Cabaleiro-lago, F. Quinlan-pluck, I. Lynch, S. Lindman, A. M. Minogue, E. Thulin, D. M. Walsh, K. A. Dawson and S. Linse, *J. Am. Chem. Soc.*, 2008, **130**, 15437.
- 24 C. Måansson, P. Arosio, R. Hussein, H. H. Kampinga, R. M. Hashem, W. C. Boelens, C. M. Dobson, T. P. J. Knowles, S. Linse and C. Emanuelsson, *J. Biol. Chem.*, 2014, **289**, 31066.
- 25 M. F. M. Sciacca, V. Romanucci, A. Zarrelli, I. Monaco, F. Lolicato, N. Spinella, C. Galati, G. Grasso, L. D'Urso, M. Romeo, L. Diomedè, M. Salmona, C. Bongiorno, G. Di Fabio, C. La Rosa and D. Milardi, *ACS Chem. Neurosci.*, 2017, **8**, 1767.
- 26 L. Yang, J. Sun, W. Xie, Y. Liu and J. Liu, *J. Mater. Chem. B*, 2017, **5**, 5954.
- 27 A. Aliyan, T. J. Paul, B. Jiang, C. Pennington, G. Sharma, R. Prabhakar and A. A. Martí, *Chem.*, 2017, **3**, 898.
- 28 Y. Ishida, S. Tanimoto, D. Takahashi and K. Toshima, *Med. Chem. Commun.*, 2010, **1**, 212.
- 29 Y. Ishida, T. Fujii, K. Oka, D. Takahashi and K. Toshima, *Chem.-Asian J.*, 2011, **6**, 2312.
- 30 M. Li, C. Xu, J. Ren, E. Wang and X. Qu, *Chem. Commun.*, 2013, **49**, 11394.
- 31 J. S. Lee, B. I. Lee and C. B. Park, *Biomaterials*, 2015, **38**, 43.
- 32 A. Taniguchi, D. Sasaki, A. Shiohara, T. Iwatsubo, T. Tomita, Y. Sohma and M. Kanai, *Angew. Chem., Int. Ed.*, 2014, **53**, 1382.
- 33 A. Taniguchi, Y. Shimizu, K. Oisaki, Y. Sohma and M. Kanai, *Nat. Chem.*, 2016, **8**, 974.
- 34 D. Osaki and H. Hiramatsu, *Amyloid*, 2016, **23**, 234.
- 35 M. Suzuki and T. Miura, *Biochim. Biophys. Acta*, 2015, **1848**, 753.
- 36 H. Okada, T. Komuro, T. Sakai, Y. Matsuo, Y. Ono, K. Omote, K. Yokoo, K. Kawachi, Y. Kasama, S. Ono, R. Hatakeyama, T. Kaneko and H. Tobita, *RSC Adv.*, 2012, **2**, 10624.
- 37 R. W. Redmond and J. N. Gamlin, *Photochem. Photobiol.*, 1999, **70**, 391.
- 38 K. Duff, C. Eckman, C. Zehr, X. Yu, C. M. Prada, J. Perez-tur, M. Hutton, L. Buee, Y. Harigaya, D. Yager, D. Morgan, M. N. Gordon, L. Holcomb, L. Refolo, B. Zenk, J. Hardy and S. Younkin, *Nature*, 1996, **383**, 710.
- 39 H. Hiramatsu, H. Ochiai and T. Komuro, *Chem. Biol. Drug Des.*, 2016, **87**, 425.
- 40 S. Leach, M. Vervloet, A. Després, E. Bréheret, J. P. Hare, T. J. Dennis, H. W. Kroto, R. Taylor and D. R. M. Walton, *Chem. Phys.*, 1992, **160**, 451.
- 41 X. Chang and P. J. Vikesland, *Langmuir*, 2013, **29**, 9685.
- 42 P. D. Q. Huy and M. S. Li, *Phys. Chem. Chem. Phys.*, 2014, **16**, 20030.
- 43 L. Xie, Y. Luo, D. Lin, W. Xi, X. Yang and G. Wei, *Nanoscale*, 2014, **6**, 9752.
- 44 K. Murakami, K. Irie, A. Morimoto, H. Ohigashi, M. Shindo, M. Nagao, T. Shimizu and T. Shirasawa, *Biochem. Biophys. Res. Commun.*, 2002, **294**, 5.
- 45 F. Chiti, M. Stefani, N. Taddei, G. Ramponi and C. M. Dobson, *Nature*, 2003, **424**, 805.
- 46 M. Palmlad, A. Westlind-Danielsson and J. Bergquist, *J. Biol. Chem.*, 2002, **277**, 19506.
- 47 B. Zhao, Y.-Y. He, P. J. Bilski and C. F. Chignell, *Chem. Res. Toxicol.*, 2008, **21**, 1056.
- 48 Z. Hu, C. Zhang, Y. Huang, S. Sun, W. Guan and Y. Yao, *Chem.-Biol. Interact.*, 2012, **195**, 86.

